PHYSICAL REVIEW C **85**, 034318 (2012)

Microscopic cluster description of ^{12}C

V. Vasilevsky*
Bogolyubov Institute for Theoretical Physics, Kyiv, Ukraine

F. Arickx,† W. Vanroose,‡ and J. Broeckhove§
Departement Wiskunde-Informatica, Universiteit Antwerpen, Antwerpen, Belgium
(Received 8 January 2012; revised manuscript received 21 February 2012; published 19 March 2012)

We investigate both bound and resonance states in ^{12}C embedded in a three-α-cluster continuum using a three-cluster microscopic model. The model relies on the hyperspherical harmonics basis to enumerate the channels describing the three-cluster discrete and continuous spectrum states. It yields the most probable distribution of the three α clusters in space, and the dominant decay modes of the three-cluster resonances.

DOI: 10.1103/PhysRevC.85.034318 PACS number(s): 21.60.Gx, 26.20.Fj, 25.55.Ci

I. INTRODUCTION

The ^{12}C nucleus is an interesting example of the so-called Borromean nuclei, as it has no bound states in any two-cluster subsystem of its three-cluster configuration. The lowest dissociation threshold (7.276 MeV above the ground state) is that of a three-α-particle disintegration. This three-cluster configuration is thus responsible to a great extent for the formation of a few bound, and many resonance states. The next threshold is of a two-cluster nature: $^{11}B + p$ [1]. It opens when the excitation energy of ^{12}C exceeds 15.96 MeV. One therefore expects only a negligible influence of the latter channel on the bound and resonance states of ^{12}C in the vicinity of the $\alpha + \alpha + \alpha$ threshold.

The ^{12}C nucleus is unique because of its excited "Hoyle state." This state is important in the context of the nucleosynthesis of carbon in helium-burning red giant stars. It is a 0^+ state with an energy of 7.65 MeV above the ground state, or 0.4 MeV above the three-cluster $\alpha + \alpha + \alpha$ threshold. Its width is only 8.5 eV, indicating a long lifetime. One immediately relates this to the 0^+ state in ^{8}Be described by two α particles, with an energy of 0.092 MeV above the $\alpha + \alpha$ threshold, and a width of 5.57 eV.

Many efforts have been made to reproduce the experimentally observed structure of ^{12}C, and to explore and understand the nature of the ground, excited, and resonance states. This was, for example, done within so-called semimicroscopic models (considering structureless α particles) [2–8] and within fully microscopic models [9–24].

A somewhat general feature of the calculations is that, with potentials which adequately reproduce the α-α interaction (this includes the phase shifts for 0^+, 2^+, and 4^+ states, and the position of the corresponding resonance states), one obtains a noticeably overbound ground state for ^{12}C.

To determine the energies and widths of the resonance states created by a three-cluster continuum, only a few methods can be used. One popular method for obtaining the resonance properties in many-cluster, many-channel systems is the complex scaling method (see reviews [25,26] and references therein). Other methods start from a calculated form of the S matrix in a wide energy range, and determine the resonance states as the pole(s) of the S matrix. The advantage of these methods is that they provide the scattering quantities (such as phase shifts, cross sections, etc.) and the resonance properties (energies and widths), as well as the wave functions of scattering and resonance states. The latter then allow one to obtain more information about the nature of the resonance states.

^{12}C is known from theory and experiment (see, e.g., [32] and [33]) to have some very narrow resonances above the three-α threshold. One may wonder why a system with several open channels does not decay instantly, but manifests these narrow resonance states. There are two possible answers to this question. First, a resonance state appears in one single channel of the multichannel system. Such particular channel is usually weakly coupled to a number, or all, of the other open channels. It is well known that this weak coupling of channels predetermines the existence of long-lived resonance states. Second, a resonance can be more or less uniformly distributed over all open channels, and the compound system needs (some) time for the resonance to be accumulated by one or a few numbers of open channels to decay into. Such a distribution over many open channels leads to very narrow resonances, as was predicted by A. Baz' [31]. It is referred to as diffusionlike processes in scattering. This type of resonance is attributed to the effect that "the system spends most of its time wandering from one channel to another" [31].

In this paper we wish to calculate and analyze the bound and continuum structure of ^{12}C, and gain some insight in the nature of these states. Indeed, in some publications (e.g., [27–30]) the suggestion for a dominant linear, chainlike, three-cluster structure appears for some of the ^{12}C resonances. We will look for confirmation of this structure. To this end, we determine the most probable configuration of the three α particles both in coordinate and momentum space. We also qualify those channels on which the resonance states of ^{12}C preferentially decay.

*VSVasilevsky@gmail.com
†Frans.Arickx@ua.ac.be
‡Wim.Vanroose@ua.ac.be
§Jan.Broeckhove@ua.ac.be

The main results of this paper are obtained by applying the "algebraic model in a hyperspherical harmonics basis" (AMHHB) [34–36] on a configuration of three α particles. In this model the three clusters are treated equally, and their relative motion described by hyperspherical harmonics. The latter enumerate the channels of the three-cluster continuum and allow one to implement the correct boundary conditions for the three-cluster exit channels. The AMHHB was applied successfully to study resonances in nuclei with a large excess of protons or neutrons such as ^{6}He, ^{6}Be, ^{5}H. The method provides the energies and widths of the resonances, and their total and partial widths, as well as the corresponding wave functions. The latter allow one to analyze the nature of the resonance states. The results of this model are compared to those obtained in other, more or less comparable, microscopic descriptions from the literature, and to experiment.

In the next section we elaborate on the method used to calculate the spectrum of ^{12}C. Section III focuses on the results obtained using this method. We also present correlation functions and density functions to characterize more precisely the spatial configuration of the three α particles for specific resonance states. We also compare the results to those of other microscopic calculations as well as to experiment.

II. THE MICROSCOPIC CLUSTER MODEL

In this section we describe the microscopic model used to determine the structure of ^{12}C in the present paper. As it has already been introduced and used in several publications, we will limit ourselves to the most important notations and aspects of importance to the current calculations.

A. The three-cluster AMHHB model

The three-cluster "algebraic model in a hyperspherical harmonics basis" (AMHHB) [34–37] will be applied to a single $^{12}\mathrm{C} = \alpha + \alpha + \alpha$ three-cluster configuration.

This model takes a hyperspherical harmonics basis (HH) to characterize and enumerate the different three-cluster channels. In each of these channels an oscillator basis describes the radial behavior, and is used to expand the many-particle wave function. A matrix version of the Schrödinger equation is obtained after substitution of this wave function. It is solved by the algebraic method (also called the modified J-matrix method [36]) for both bound and scattering states using the correct asymptotics.

A similar approach, using the hyperspherical harmonics, was proposed in [39,40] in coordinate representation, using the generator coordinate technique to solve the corresponding Schrödinger equation.

The AMHHB wave function for ^{12}C is written as

$$\begin{aligned}\Psi &= \widehat{\mathcal{A}}\{\Phi(\alpha_1)\Phi(\alpha_2)\Phi(\alpha_3) f(\mathbf{x},\mathbf{y})\} \\ &= \widehat{\mathcal{A}}\{\Phi(\alpha_1)\Phi(\alpha_2)\Phi(\alpha_3) f(\rho,\theta;\widehat{\mathbf{x}},\widehat{\mathbf{y}})\} \\ &= \sum_{n_\rho,K,l_1,l_2} C_{n_\rho,K,l_1,l_2} |n_\rho, K, l_1, l_2; LM; (\rho,\theta;\widehat{\mathbf{x}},\widehat{\mathbf{y}})\rangle, \end{aligned} \quad (1)$$

where $|n_\rho, K, l_1, l_2; LM\rangle$ is a cluster oscillator function [34]:

$$\begin{aligned}|n_\rho, K, l_1, l_2; LM\rangle = \widehat{\mathcal{A}}\{&\Phi(\alpha_1)\Phi(\alpha_2)\Phi(\alpha_3) R_{n_\rho,K}(\rho) \\ &\times \chi_{K,l_1,l_2}(\theta)\{Y_{l_1}(\widehat{\mathbf{y}})Y_{l_2}(\widehat{\mathbf{x}})\}_{LM}\}. \end{aligned} \quad (2)$$

These functions are enumerated by the number of hyperradial excitations n_ρ, hyperspherical momentum K, and two partial orbital momenta l_1, l_2. The vectors $\mathbf{x}$ and $\mathbf{y}$ form a set of Jacobi coordinates, and ρ and θ are hyperspherical coordinates, related to the Jacobi vectors by

$$\rho = \sqrt{\mathbf{x}^2 + \mathbf{y}^2}, \quad |\mathbf{x}| = \rho\cos\theta, \quad |\mathbf{y}| = \rho\sin\theta. \quad (3)$$

The notation $\widehat{\mathbf{x}}$ and $\widehat{\mathbf{y}}$ refers to unit length vectors. Vector $\mathbf{x}$ corresponds to the distance between two selected α particles, with an associated partial orbital angular momentum l_2. Vector $\mathbf{y}$ is the displacement of the third α particle with respect to the center of mass of the other two, with an associated angular momentum l_1. The three quantum numbers $c = \{K, l_1, l_2\}$ determine the channels of the three-cluster system in the AMHHB.

The fact that all three clusters are identical leads to some specific issues. The wave function (1) for ^{12}C is antisymmetric with respect to the permutation of any pair of nucleons. Because the three clusters are identical, this function should be symmetric with respect to the permutation of any pair of α particles. This imposes constraints on the allowed quantum numbers of the wave function. Because of this symmetry, for instance, the partial orbital momentum l_2 of a two-cluster subsystem can only have even values. As the parity of ^{12}C states is defined as $\pi = (-1)^{l_1+l_2}$, it is fully determined by the partial orbital angular momentum l_1 of the relative motion of the remaining cluster with respect to the two-cluster subsystem.

In [12,41] it was suggested to use a symmetrization operator to construct the proper basis states. For a discussion on the symmetry of a system with three identical clusters we refer to [42].

The symmetrical hyperspherical harmonics basis for a three-particle system was realized many years ago (see, e.g., [43,44]). An explicit form of a few basis functions for small values of the total angular momentum ($L = 0$, 1, and 2) can be derived. However it is extremely intricate to use for explicit calculation of matrix elements.

An alternative approach to obtain such matrix elements without an explicit realization of the basis functions consists in using the generating function technique. One can indeed construct a generating function for the overlap and Hamiltonian kernels of ^{12}C, using the procedure explained in [34], that satisfies all required symmetry conditions, including the cluster symmetric permutation behavior. Explicit matrix elements of the operators can then be obtained by using recurrence relations. The standard approach in the AMHHB is to extract matrix elements characterized by explicit l_1, l_2 quantum numbers. These, however, do not yet correspond to the desired symmetrical harmonics. Indeed, the states $|n_\rho, K, l_1, l_2; LM\rangle$ for fixed n_ρ and K do not belong to the desired symmetrical irreducible representation of S(3), the permutation group of the three α clusters, with the Young tableau [3]. They are, in fact, linear combinations of the Young

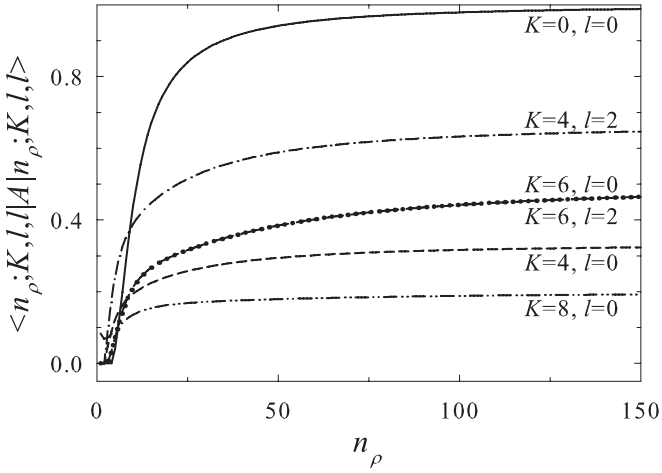

FIG. 1. Matrix elements of the antisymmetrization operator in the unsymmetrized hyperspherical basis ($K = 6, l = 0$ and $K = 6, l = 2$ coincide).

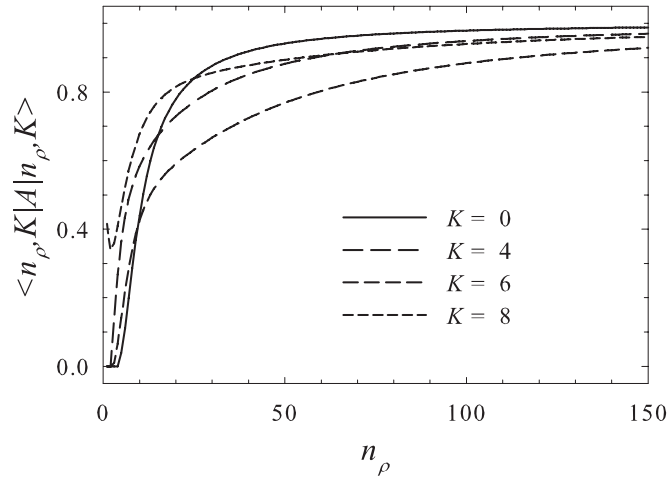

FIG. 2. Matrix elements of the antisymmetrizator in the symmetrized hyperspherical basis.

tableau [3] and the nonsymmetrical Young tableaus [1,2] and [111].

The antisymmetrization operator in the standard AMHHB basis has nonzero matrix elements,

$$\langle n_\rho, K, l_1, l_2; LM|\widehat{A}|\widetilde{n}_\rho, \widetilde{K}, \widetilde{l}_1, \widetilde{l}_2; LM\rangle, \tag{4}$$

for fixed oscillator shells with $N_{sh} = 2\,n_\rho + K = 2\,\widetilde{n}_\rho + \widetilde{K}$. By selecting only the matrix elements with hyperradial quantum number $n_\rho = \widetilde{n}_\rho$ and hypermomentum $K = \widetilde{K}$, one obtains relatively small matrices whose eigenfunctions $|n_\rho, K, \nu; LM\rangle$ with nonzero eigenvalues are of the correct symmetrical hyperspherical type, because of the symmetry properties of the generating function. Index ν (1,2,...) enumerates the symmetrical hyperspherical harmonics for a given value of the hypermomentum K.

This procedure is similar to the procedure of obtaining the Pauli allowed states in three-cluster systems (for details see [45]).

This is demonstrated in Fig. 1 where the diagonal matrix elements of the antisymmetrization operator between the original hyperspherical harmonics are displayed for total angular momentum $L = 0$, for all channels up to $K = 8$. One notices that the matrix elements,

$$\langle n_\rho, K, l_1 = l_2; L = 0|\widehat{A}|n_\rho, \quad K, l_1 = l_2; L = 0\rangle, \tag{5}$$

do not tend to unity, as one could expect, but to some fixed values. Analysis shows that these asymptotic values of (5) correspond to the weights of the symmetrized hyperspherical harmonics with the Young tableau [3], within the original harmonic.

The eigenvalues obtained after diagonalization, however, which are matrix elements of symmetrized harmonics, do display the correct asymptotic behavior (i.e., all tend to unity), as can be seen in Fig. 2.

In Table I we display both the total number of (original) nonsymmetrized and symmetrized channels for different values of the total orbital momentum. The symmetrization significantly reduces the number of channels compatible with the maximal value of hypermomentum $K_{\max}$. Only even values of the partial orbital momentum l_2 are considered because of the symmetry rules for two-cluster subsystems.

In Refs. [34,35] the importance and meaning of the effective charges $Z_{c,\tilde{c}}$ were defined in the context of the AMHHB, and explicitly discussed for the ^{6}Be nucleus in three-cluster configuration $^4\mathrm{He} + p + p$. The effective charge determines the asymptotic form of the three-cluster potential originating from the Coulomb interaction, which has the form,

$$V^{(C)}_{c,\tilde{c}} = \frac{Z_{c,\tilde{c}}}{\rho} \tag{6}$$

It was shown that it is of crucial importance for implementing the correct boundary conditions for the three-cluster continuum states.

The symmetrization influences the behavior of the effective charges. In Table II we display the effective charges for the 0^+ state of ^{12}C, calculated in the original, nonsymmetrized, basis of the hyperspherical harmonics, for $K_{\max} = 8$. One easily verifies that they coincide with those calculated in Ref. [23].

In Table III we display the effective charges in the symmetrized basis. Only four channels remain after symmetrization. In particular no $K = 2$ channel remains, so we omitted these also in Table II even though they have a nonzero contribution.

It goes without saying that the asymptotic form of the effective three-cluster potential which originates from the nucleon-nucleon interaction [34],

$$V^{(NN)}_{c,\tilde{c}} = \frac{V_{c,\tilde{c}}}{\rho^3}, \tag{7}$$

TABLE I. Number of channels for unsymmetrized and symmetrized hyperspherical harmonics (enumerated by ν for given K).

J^π	0^+	2^+	4^+	1^-	3^-
$K_{\max}$	14	14	14	13	13
N_{ch} ($\{K, l_1, l_2\}$)	20	44	54	28	42
N_{ch} ($\{K, \nu\}$)	8	16	19	9	14

TABLE II. Effective charges for the $J^\pi = 0^+$ state of ^{12}C.

(K, l_1, l_2)	(0,0,0)	(4,0,0)	(4,2,2)	(6,0,0)	(6,2,2)	(8,0,0)	(8,2,2)	(8,4,4)
(0,0,0)	28.81	2.47	3.49	2.74	−2.74	0.87	0.00	1.04
(4,0,0)	2.47	32.157	−1.13	3.95	−0.31	4.67	0.00	1.95
(4,2,2)	3.49	−1.13	31.35	1.72	−4.30	0.00	0.66	0.00
(6,0,0)	2.74	3.95	1.72	33.48	−2.51	4.63	0.00	0.45
(6,2,2)	−2.74	−0.31	−4.30	−2.51	34.29	0.00	0.62	0.00
(8,0,0)	0.87	4.67	0.00	4.63	0.00	34.29	0.00	−2.38
(8,2,2)	0.00	0.00	0.66	0.00	0.62	0.00	33.08	0.00
(8,4,4)	1.04	1.95	0.00	0.45	0.00	−2.38	0.00	32.41

is also influenced by the symmetrization. This asymptotic component is very important for obtaining the correct values of the S matrix. We do not dwell on its explicit form here, but apply a procedure similar to that for the effective charges.

B. Phases, eigenphases, and resonances

After solving the system of linear equation of the AMHHB model, we obtain the wave functions of the continuous spectrum states, and the scattering S matrix. We consider two different representations of the S matrix.

In the first representation, the elements of the S matrix are described through the phase shifts δ_{ij} and the inelastic parameters η_{ij}:

$$S_{ij} = \eta_{ij} \exp(2i\delta_{ij}), \tag{8}$$

of which one usually only analyzes the diagonal matrix elements by displaying the δ_{ii} and η_{ii} quantities. In the second representation the S matrix is reduced to diagonal form, leading to the so-called eigenphases, which now represent the elastic scattering of the many-channel system in independent (uncoupled) eigenchannels:

$$\|S\| = \|U\|^{-1}\|D\|\|U\|. \tag{9}$$

Here $\|U\|$ is an orthogonal matrix, connecting both representations, and $\|D\|$ is a diagonal matrix with nonzero elements,

$$D_{\alpha\alpha} = \exp(2i\delta_\alpha), \tag{10}$$

defining the eigenphases δ_α.

The phases shifts δ_{ii}, inelastic parameters η_{ii} and eigenphases δ_α then provide sufficiently detailed information about the channels that are involved in the production of resonance states. The eigenphases are used to extract the resonance positions and total widths in the traditional way,

$$\left.\frac{d^2\delta_\alpha}{dE^2}\right|_{E=E_r} = 0, \quad \Gamma = 2\left(\left.\frac{d\delta_\alpha}{dE}\right|_{E_r}\right)^{-1}, \tag{11}$$

whereas the orthogonal matrix $\|U\|$ leads to the partial decay widths of the resonance (for details see, e.g., [36]).

TABLE III. Effective charges for the $J^\pi = 0^+$ state of ^{12}C for symmetrized channels.

(K, ν)	(0,1)	(4,1)	(6,1)	(8,1)
(0,1)	28.810	4.277	3.880	1.139
(4,1)	4.277	30.556	5.217	2.301
(6,1)	3.880	5.217	35.990	1.457
(8,1)	1.139	2.301	1.457	31.450

C. Correlation functions and density distributions

As we pointed out, the AMHHB model allows one to calculate the scattering properties, but also to obtain the wave function at any energy, in particular, at the resonance positions. The latter is of the utmost importance to analyze the nature of the system at these energies.

Within the AMHHB model the solution is fully expressed by the expansion coefficients $\{C_{n_\rho,c}\}$ and the S matrix. The expansion coefficients $\{C_{n_\rho,c}\}$ determine both the total three-cluster wave function of a compound system Ψ, as well as the wave function of the relative motion of three clusters $f(\mathbf{x}, \mathbf{y})$ [see Eq. (1)].

The latter contains all information on the dynamic behavior of the three-cluster system for bound as well as continuum states. It is interesting to note that these coefficients are identical in both the representations of the wave function in coordinate and momentum space, because of the Fourier transform properties of the oscillator states. The wave function $f(\mathbf{k}, \mathbf{q})$ in momentum space has arguments that are directly related to the coordinate representation: $\mathbf{k}$ is the momentum of relative motion of two clusters, whereas $\mathbf{q}$ is the momentum of the third cluster with respect to the center of mass of the two-cluster subsystem.

We obtain the density distribution in coordinate space as

$$D(x, y) = D(\rho, \theta) = \int |f(\mathbf{x}, \mathbf{y})|^2 d\hat{\mathbf{x}} d\hat{\mathbf{y}}, \tag{12}$$

and the corresponding correlation function as

$$C(x, y) = C(\rho, \theta) = x^2 y^2 \int |f(\mathbf{x}, \mathbf{y})|^2 d\hat{\mathbf{x}} d\hat{\mathbf{y}}, \tag{13}$$

directly from the wave function of relative motion $f(\mathbf{x}, \mathbf{y})$. Both the density distribution and correlation function in momentum space are obtained in the same way using the wave function of relative motion in momentum space $f(\mathbf{k}, \mathbf{q})$.

In a calculation with $N_{\rm ch}$ open channels, one obtains $N_{\rm ch}$ independent wave functions describing the elastic and inelastic

processes in the many-channel system. It is quite impossible to analyze all of these wave functions when many channels are open. Some principles have to be set up on how to select the most important wave functions. In Ref. [36] we formulated some criteria for selecting the dominant wave function of a resonance. We will use the same criteria in this paper to select the "resonance wave functions."

III. CALCULATIONS AND RESULTS

In the present calculations for ^{12}C we consider for the nucleon-nucleon interaction the Minnesota potential [46]. The oscillator basis is characterized by an oscillator length $b = 1.2846$ fm, to minimize the ground-state energy of the α particle using the above potential.

Parameter u of the Minnesota potential is taken to be $u = 0.94$ to reproduce the phase shifts for $\alpha + \alpha$ scattering, and the 0^+, 2^+, and 4^+ resonances in ^{8}Be. The same parameters were used by Arai [17].

The $^8\text{Be} = \alpha + \alpha$ two-cluster substructure is of key importance in the description of ^{12}C. We present $\alpha + \alpha$ resonance properties in Table IV. The AMOB model (algebraic model using an oscillator basis) takes a set of oscillator functions to describe the intercluster behavior, and the algebraic model to obtain the phase shifts for $\alpha + \alpha$ scattering (see, e.g., [47]). We include a comparison to the results of Arai in his paper on ^{12}C [17], where he uses the "analytical continuation of the S matrix to the complex plane" method to obtain the resonance characteristics.

These results form a first test of the consistency of the different expansion methods used, applied to the two-cluster subsystem. Although quite similar, one still notices that the resonance properties of the two-cluster $\alpha - \alpha$ system have a slight dependence on the method used.

A. The potential and Coulomb interaction in AMHHB

In Figs. 3 and 4 the diagonal matrix elements of the nucleon-nucleon and Coulomb interactions within the AMHHB model are displayed, again for channels up to $K = 8$. One observes that the nucleon-nucleon interaction creates a deep potential well with a long tail in the hyperspherical coordinate. This tail reflects the asymptotic form of the potential, indicated in Eq. (7). The matrix elements of the Coulomb interaction indicate the magnitude of the Coulomb barrier, which is the main factor for generating the resonance states in ^{12}C.

TABLE IV. Resonance properties for ^{8}Be obtained with different methods.

J^π	AMOB (see text)		Arai [17]	
	E, MeV	Γ, keV	E, MeV	Γ, MeV
0^+	0.022	$6.30\ 10^{-10}$	0.03	$<10^{-6}$
2^+	2.93	1.51	2.9	1.4
4^+	12.55	5.01	12.5	4.8

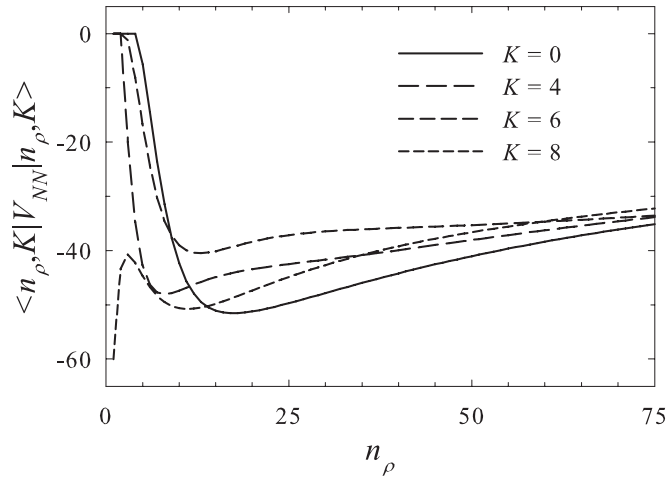

FIG. 3. Diagonal matrix elements of $\widehat{V}_{NN}$ between symmetrized hyperspherical harmonics.

B. Phase shifts and eigenphases

In Fig. 5 we show results of the AMHHB calculations for the 2^+ state in terms of the symmetrical hyperspherical harmonic channels through the (diagonal) phase shifts δ_{ii} and the inelastic parameters η_{ii}.

The scattering parameters are obtained from a calculation with maximal hypermomentum $K_{\max} = 14$. One observes from Fig. 5 that for small energies the channels are totally uncoupled ($\eta_{ii} \approx 1$). A first 2^+ resonance appears at $E = 2.731$ MeV, and is mainly produced in the first channel with hypermomentum $K = 2$, whereas a second resonance at energy $E = 3.113$ MeV is dominated by hypermomentum $K = 4$. The inelastic parameters for the first two channels have a pronounced minimum at the energy of the first resonance, and a shallow minimum at the second resonance energy. In addition, the first resonance displays a "shadow resonance" behavior in the second channel. This is a typical behavior for resonances in a many-channel system (see, for instance, the detailed analysis of two-channel resonances in ^{5}He in [48]).

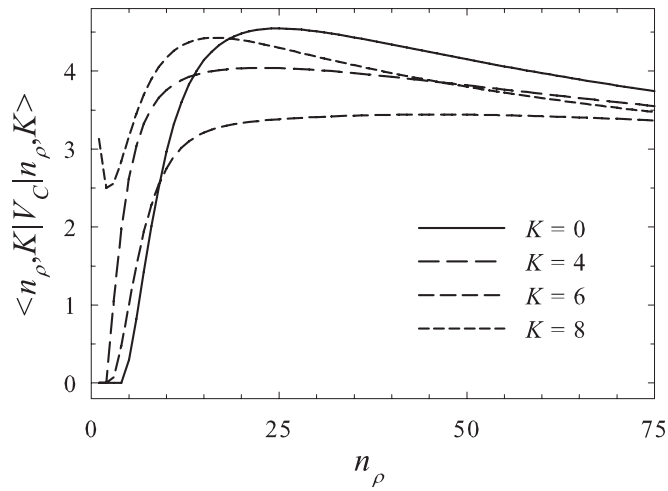

FIG. 4. Diagonal matrix elements of $\widehat{V}_C$ between symmetrized hyperspherical harmonics.

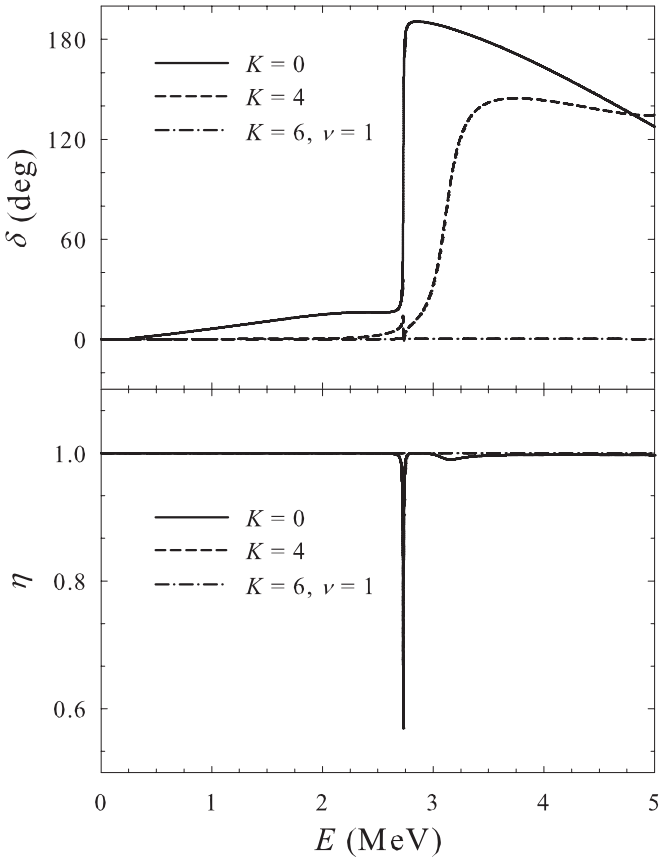

FIG. 5. Diagonal phase shifts and inelastic parameters for the $J^\pi = 2^+$ state.

The minimum in the inelastic parameters indicates that the compound system is being reconstructed at this energy, and transits from one channel to another.

In Fig. 6 we display the corresponding eigenphase shifts δ_α for the first three eigenchannels. One observes now that both resonance states are mainly associated with the first eigenchannel, and that the second eigenchannel only contributes marginally.

C. Convergence properties

A convergence study of the energies (and widths) for bound and resonance states should indicate whether the Hilbert space is sufficiently large for stable and reliable results. The AMHHB model space is characterized by two parameters: the maximal value of hypermomentum $K_{\max}$, and the maximal value of the hyperradial excitation $n_{\rho_{\max}}$. Usually the choice is a compromise between the convergence of the results and the computational burden. A set of hyperspherical harmonics with $K_{\max} = 14$ for even parity states, and $K_{\max} = 13$ for odd parity states, seems sufficient and remains computationally feasible. This choice accounts for a large number of three-cluster configurations or, in other words, for a sufficient number of inherent (triangular) shapes for the three clusters. We refer to Ref. [38] for examples of most probable triangular shapes for the hyperspherical harmonics from $K = 0$ to $K = 10$.

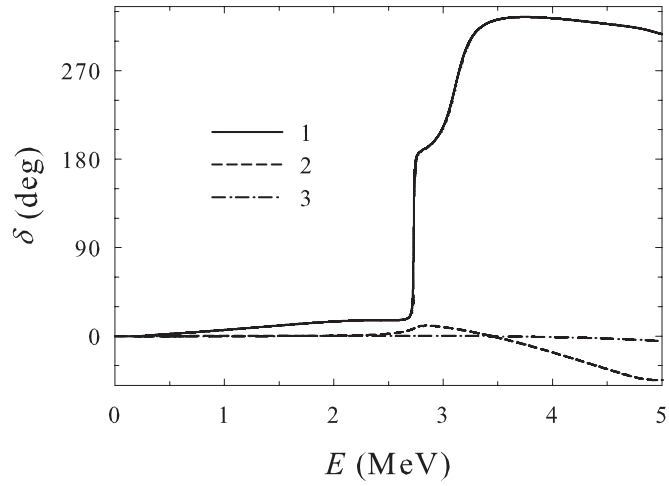

FIG. 6. Eigenphase shifts for $J^\pi = 2^+$ for the first three eigenchannels.

A first convergence test considers the 0^+, 2^+, and 4^+ bound states of ^{12}C, shown in Fig. 7 as a function of $K_{\max}$. One observes that the deeply bound states ($J^\pi = 0^+, 2^+$) require significantly less hyperspherical harmonics for a converged energy than the shallow, or weakly bound, state with $J^\pi = 4^+$. At least all hyperspherical harmonics with $K_{\max} \geqslant 6$ are required to bind the latter state, whereas for $J^\pi = 0^+$ one already obtains binding with a single hyperspherical harmonic with $K = 0$. Figure 7 further demonstrates that the above choice of $K_{\max}$ amply leads to sufficient precision for the bound states.

In Table V we turn to the energies and widths of the 0^+ and 2^+ resonances obtained with increasing number of hyperspherical harmonics. One observes that sufficient convergence of the resonances occurs at $K_{\max} = 12$. It is furthermore interesting to note that these resonances already appear with reasonable energy and width values when only the lowest channel ($K = 0$ for the 0^+ state and $K = 2$ for the 2^+ state) is considered. This is a remarkable result for ^{12}C, as, for

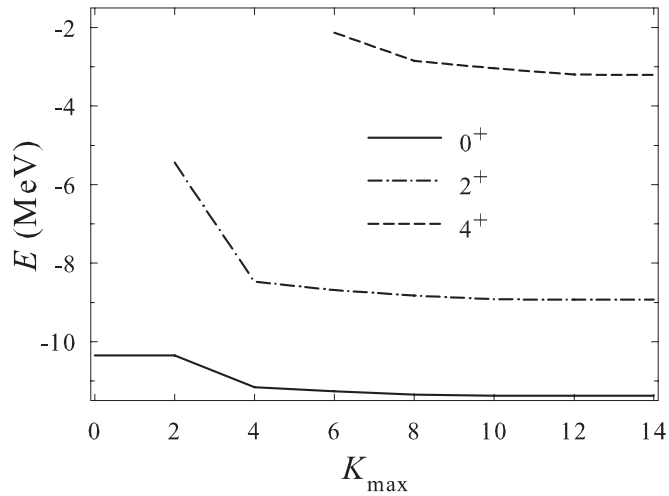

FIG. 7. Convergence of the bound states in AMHHB.

TABLE V. Energy (MeV) and width (keV) of the low-lying resonances in terms of $K_{\max}$.

L^π	$K_{\max}$	0	4	6	8	10	12	14
0^+	E	0.40	0.75	0.74	0.72	0.70	0.68	0.68
	Γ	205.08	13.40	11.79	7.10	4.35	2.71	2.78
0^+	E	1.15	7.34	6.09	5.55	5.54	5.16	5.14
	Γ	510.16	897.64	422.50	539.21	586.08	534.33	523.46
2^+	E	–	3.28	2.89	2.83	2.78	2.74	2.73
	Γ	–	30.19	13.07	11.85	9.95	8.84	8.75
2^+	E	–	3.50	3.27	3.22	3.17	3.14	3.11
	Γ	–	274.51	351.57	308.29	280.23	263.80	246.78

example, for ^{6}Be it was impossible to generate a 0^+ resonance with a single $K = 0$ channel (see Ref. [35]).

In all calculations we have considered states with hyperradial excitation up to $n_{\rho\,\max} = 70$, which covers a large range of intercluster distances, and reaches well into the asymptotic region.

D. Partial widths

In Table VI we display the energy, the total width (Γ), and the partial widths ($\Gamma_i, i = 1, 2, \ldots$) in the corresponding decay channels for the even parity resonances, and in Table VII for the odd parity resonances.

One observes that in most cases only one or two channels are responsible for the decay of the resonance states. The remaining channels contribute negligibly, and the corresponding partial width does not exceed 10^{-5} keV. Only for the 4^+ resonance a significant distribution over multiple channels is apparent.

One should note that, although the resonances are created by only a few channels, the role of the other, very weakly coupled, channels is still important. This can be seen from Table V for the first 0^+ resonance: It is indeed generated mainly by the channel with minimal hypermomentum $K = 0$, but modified substantially with increasing number of hypermomentum. The same applies to the other resonance states.

E. Correlation functions and density distributions

In Fig. 8 we show the correlation function for the ^{12}C ground state, and observe that this state displays a compact spatial configuration, as it is expected for such a deeply bound state. The most probable shape of the three α-cluster system is an almost equilateral triangle with a distance between any two α particles of approximately 3 fm.

The correlation function for the first 0^+ resonance state on the other hand, shown in Fig. 9, shows a more deformed system with two α particles relatively close to one another (about 3.5 fm) and the third α particle further away (approximately 5 fm). So ^{12}C features a prolate triangle as a dominant configuration for this state.

One also observes on Fig. 9 a small maximum for the correlation function corresponding to an almost linear configuration of three α particles, two of them being approximately 4 fm apart, and the third 0.2 fm away from their center of mass. However, the weight of this linear configuration is approximately 6 times less than the weight of the prolate triangular configuration. Our calculations therefore do not agree with other authors advancing a dominant linear structure [27–30].

In Fig. 10 we display the correlation function of the first resonance state in momentum space. One observes a huge maximum corresponding to relatively slowly moving α particles. A small maximum corresponding to faster moving α particles is also present.

F. Comparison to the literature

We now compare the AMHHB results to the existing literature. In Table VIII we display the AMHHB results to those of Arai [17] and Pichler *et al.* [9], both obtained by the complex scaling method (CSM). The latter authors [9] use a somewhat different value for the parameter u in the Minnesota potential, and a different oscillator length b; because of this, different results are obtained for the bound states.

Comparison with the results of Arai [17] indicates that the AMHHB model leads to resonance states with higher energy

TABLE VI. Partial widths of the even parity resonances in ^{12}C. Energy in MeV; widths in keV.

L^π	0^+		2^+		2^+		4^+	
E		0.68		2.78		3.17		5.60
Γ		2.78		9.95		280.24		0.55
Γ_1	$K = 0$	2.78	$K = 2$	6.11	$K = 2$	13.46	$K = 4$	0.23
Γ_2	$K = 4$	0	$K = 4$	3.84	$K = 4$	278.89	$K = 6$	0.15
Γ_3	$K = 6$	0	$K = 6$	$<10^{-5}$	$K = 6$	$<10^{-5}$	$K = 8$	0.16

TABLE VII. Partial widths of the odd parity resonances in ^{12}C. Energy in MeV; widths in keV.

L^π	1^-		3^-	
E		3.52		0.67
Γ		0.21		8.34
Γ_1	$K = 3$	0.206	$K = 3$	8.34
Γ_2	$K = 5$	0.002	$K = 5$	0
Γ_3	$K = 7$	$<10^{-5}$	$K = 7$	0

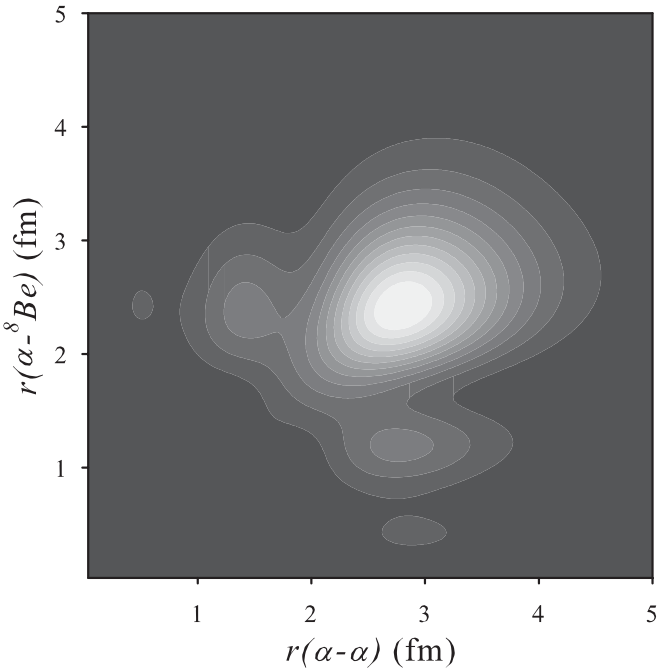

FIG. 8. Correlation function for the ^{12}C ground state in coordinate space.

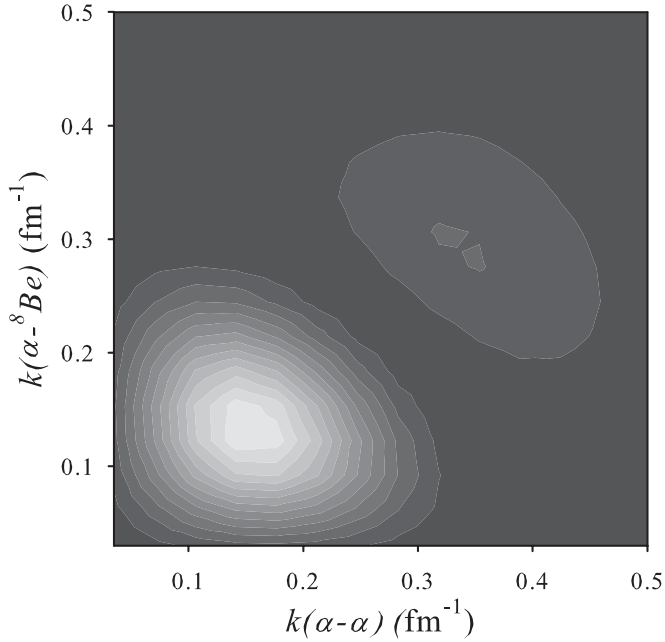

FIG. 10. Correlation function for the first 0^+ resonance state of ^{12}C in momentum space.

and smaller widths than those obtained with the CSM. This can be attributed to the difference in the methods, and to the different Hilbert spaces. Formally the Hilbert space of basis functions used by Arai [17] is quite close to the one considered in the AMHHB. Actually, in the present calculations the partial orbital momenta l_1 and l_2 are restricted by the condition,

$$L \leqslant l_1 + l_2 \leqslant K_{\max},$$

so that, for instance, for total orbital momentum $L = 0$, they run from $l_1 = l_2 = 0$ to $l_1 = l_2 = 6$ with $K_{\max} = 14$. Arai, on the other hand, restricted himself with $l_1, l_2 \leqslant 4$. In Refs. [35–37] we observed the tendency that the more hyperspherical harmonics (thus the more channels) are involved in the calculation, the smaller the resonance energy and width becomes. This tendency is again confirmed by the present AMHHB calculations. Thus some reduction of the width of the resonances, observed in our calculations with respect to Arai [17], can be attributed to the larger number of channels in our model.

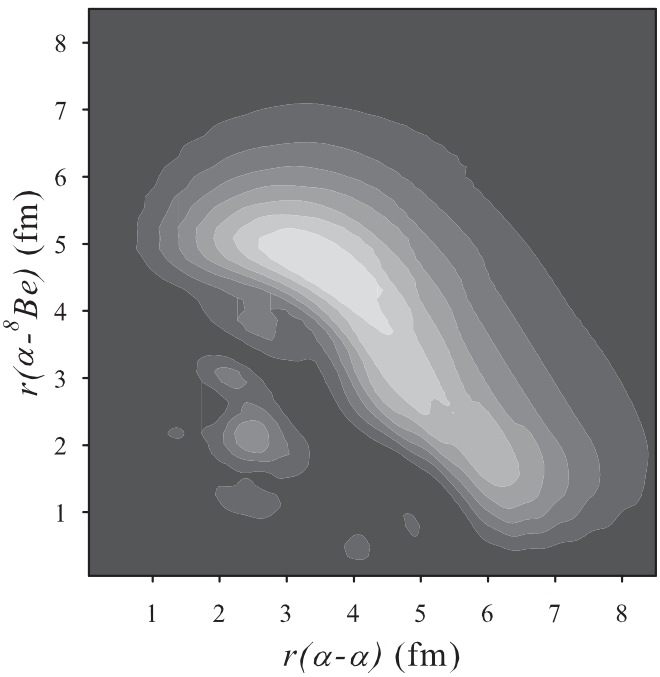

FIG. 9. Correlation function for the first 0^+ resonance state of ^{12}C in coordinate space.

TABLE VIII. Bound and resonance states of ^{12}C obtained with the AMHHB model, compared to CSM results from the literature.

Method	AMHHB		CSM-Arai		CSM-Pichler	
Reference	Present paper		[17]		*et al.* [9]	
J^π	E, MeV	Γ, keV	E, MeV	Γ, keV	E, MeV	Γ, keV
0^+	−11.372		−11.37		−10.43	
	0.684	2.78	0.4	< 1	0.64	14
	5.156	534.00	4.7	1000	5.43	920
2^+	−8.931		−8.93		−7.63	
	2.775	9.95	2.1	800	6.39	1100
	3.170	280.24	4.9	900		
4^+	−3.208		−3.21			
	5.603	0.55	5.1	2000		
1^-	3.516	0.21	3.4	200	3.71	360
3^-	0.672	8.34	0.6	<50	1.16	25
	4.348	2.89	7.1	5400	11.91	1690
	5.433	334.90	9.6	400		

TABLE IX. Bound and resonance states of ^{12}C obtained with the AMHHB model, compared to experiment.

Method Reference	AMHHB Present paper		Experiment [1]	
J^π	E, MeV	Γ, keV	E, MeV	Γ, keV
0^+	−11.372		−7.2746	
	0.684	2.78	0.3796 ± 0.0002	$(8.5 \pm 1.0) \times 10^{-3}$
	5.156	534.00	3.0 ± 0.3	3000 ± 700
2^+	−8.931		-2.8357 ± 0.0003	
	2.775	9.95	3.89 ± 0.05	430 ± 80
	3.170	280.24	8.17 ± 0.04	1500 ± 200
4^+	−3.208			
	5.603	0.55	6.808 ± 0.015	258 ± 15
1^-	3.516	0.21	3.569 ± 0.016	315 ± 25
3^-	0.672	8.34	2.366 ± 0.005	34 ± 5
	4.348	2.89		
	5.433	334.90		

Comparing the AMHHB results to the complex scaling model calculations of Pichler *et al*. [9], one observes that both yield close results for the first and second 0^+ resonance states.

On the whole one can conclude that there is consistency in the results for resonance properties in all three microscopic models.

G. Comparison to experiment

In Table IX we compare the theoretical AMHHB results for ^{12}C to available experimental data.

One notices that the first 0^+ resonance state (the Hoyle state) appears in the current calculations as a narrow resonance with an energy of 0.684 MeV and width 2.7 keV, which is considerably wider than the experimental Hoyle state (about 8.5 10^{-3} keV). This contrasts with the generally observed feature of the AMHHB calculations that the calculated widths are significantly less than the corresponding experimental widths of the ^{12}C resonances. The discrepancies between the theoretical and experimental data have essentially two origins. The first one relates to the choice of the nucleon-nucleon interaction: it was tuned to reproduce the phase shifts and resonance properties for α-α scattering. As a result it leads to overbound 0^+ and 2^+ states in ^{12}C, and binds the 4^+ state. The second one relates to the specific choice of three-cluster model and corresponding model space, as well as to the method by which the energy and width of the resonance states are obtained.

H. Optimizing the nucleon-nucleon potential

In this paper we used a Minnesota nucleon-nucleon potential tuned to reproduce the phase shifts for α-α scattering, as well as the ^{8}Be resonances. This, however, leads to overbound 0^+ and 2^+ states, and a bound 4^+ state. Moreover, the obtained resonance structure for the ^{12}C three-cluster continuum deviates from the experimentally observed one, which can also be attributed to the specific choice of semirealistic nucleon-nucleon potential.

We therefore wish to discuss the dependence of the results to the choice of parameter u on the results. To do so we use different criteria to optimize this parameter. We first determine a value to reproduce the ground-state energy of ^{12}C, followed by an attempt to reproduce the energy and width of the 0^+ Hoyle state.

In Fig. 11 we display the ground-state energy as a function of the parameter u, compared to experiment (dashed line). One observes that the ground state is reproduced with $u = 0.910$. One observes a monotonously decreasing linear dependence of the ground-state energy on u within the selected range. For the Hoyle state position and width the dependency is less trivial, as is shown in Fig. 12. One, however, observes that the value $u = 0.948$ reproduces the position of the Hoyle state, and leads to a close match for its width, too.

The correlation functions for the ground state and Hoyle state obtained with their respective optimal values were very

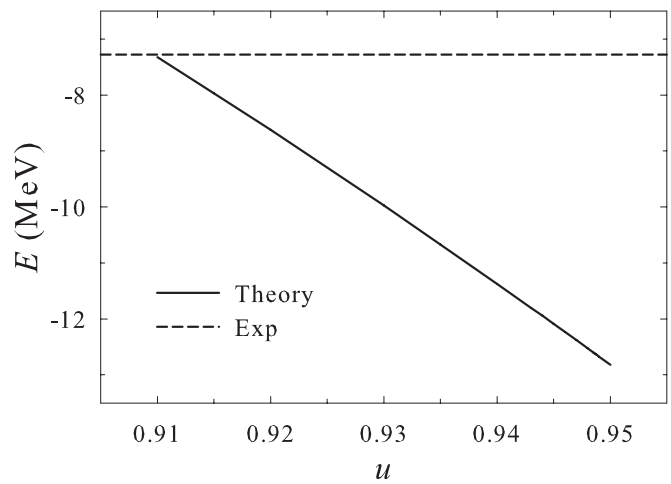

FIG. 11. Energy of the ground state as a function of parameter u of the Minnesota potential.

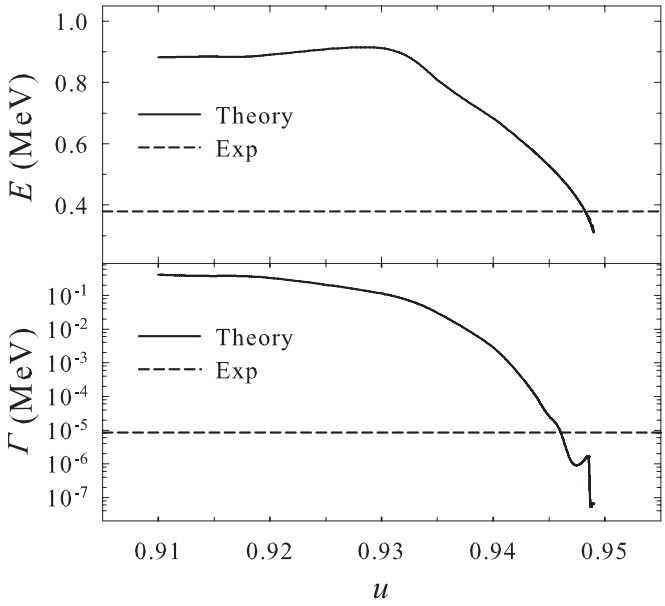

FIG. 12. Position and total width of the first 0^+ resonance state as a function of parameter u.

close to the ones obtained with the value $u = 0.94$ and displayed in Figs. 8 and 9, so that the conclusions remain unaltered.

IV. CONCLUSIONS

In this paper we described the ^{12}C nucleus with a three-cluster microscopic model.

The model correctly handles the three-cluster continuum (i.e., correctly implements the suitable boundary conditions) by using a hyperspherical harmonics basis. It leads to the scattering matrix S in many-channel space, and the energy, total, and partial widths of the resonance states and their corresponding wave functions can be obtained.

It was shown that the obtained resonances of ^{12}C agree well with other methods, and that the lowest resonances are generated by only a few number of weakly coupled channels, leading narrow resonance states. The partial widths determine the most probable channels for resonance decay. Correlation functions and density distributions revealed the dominant shape of the three-cluster triangle configuration for the lowest bound and resonance states of ^{12}C. There were no indications of a prominent linear three-cluster structure for the resonance states.

It was also shown that it is impossible to fix a unique value for the u parameter of the Minnesota nucleon-nucleon potential to fit all desired physical properties for ^{12}C, and for the disintegrating α particles. However, the qualitative conclusions remained unaltered under slight adaptation of u.

As a final conclusion we can state that the model is consistent with other microscopic models using the complex scaling methodology to determine the energy and total width of three-cluster resonance states.

ACKNOWLEDGMENTS

Support from the Fonds voor Wetenschappelijk Onderzoek Vlaanderen (FWO), Grant No. G0120-08N, is gratefully acknowledged. V. S. Vasilevsky is grateful to the Department of Mathematics and Computer Science of the University of Antwerp for hospitality. This work was supported in part by the Program of Fundamental Research of the Physics and Astronomy Department of the National Academy of Sciences of Ukraine.

[1] F. Ajzenberg-Selove, Nucl. Phys. A **506**, 1 (1990).
[2] S. I. Fedotov, O. I. Kartavtsev, V. I. Kochkin, and A. V. Malykh, Phys. Rev. C **70**, 014006 (2004).
[3] I. Filikhin, V. M. Suslov, and B. Vlahovic, J. Phys. G **31**, 1207 (2005).
[4] R. Álvarez-Rodrıguez, E. Garrido, A. S. Jensen, D. V. Fedorov, and H. O. U. Fynbo, Eur. Phys. J. A **31**, 303 (2007).
[5] R. Álvarez-Rodríguez, A. S. Jensen, D. V. Fedorov, H. O. U. Fynbo, and E. Garrido, J. Phys. Conf. Ser. **111**, 012017 (2008).
[6] R. Álvarez-Rodríguez, A. S. Jensen, E. Garrido, D. V. Fedorov, and H. O. U. Fynbo, Phys. Rev. C **77**, 064305 (2008).
[7] M. Chernykh, H. Feldmeier, T. Neff, P. von Neumann-Cosel, and A. Richter, Phys. Rev. Lett. **105**, 022501 (2010).
[8] R. de Diego, E. Garrido, D. V. Fedorov, and A. S. Jensen, Phys. Lett. B **695**, 324 (2011).
[9] R. Pichler, H. Oberhummer, A. Csótó, and S. A. Moszkowski, Nucl. Phys. A **618**, 55 (1997).
[10] C. Kurokawa and K. Katō, Nucl. Phys. A **738**, 455 (2004).
[11] Y. Fujiwara, K. Miyagawa, M. Kohno, Y. Suzuki, D. Baye, and J.-M. Sparenberg, Nucl. Phys. A **738**, 495 (2004).
[12] Y. Fujiwara, Y. Suzuki, and M. Kohno, Phys. Rev. C **69**, 037002 (2004).
[13] Y. Fujiwara, M. Kohno, and Y. Suzuki, Few-Body Syst. **34**, 237 (2004).
[14] Y. Fujiwara and H. Nemura, Prog. Theor. Phys. **107**, 745 (2002).
[15] Y. Fujiwara, K. Miyagawa, M. Kohno, Y. Suzuki, D. Baye, and J.-M. Sparenberg, Phys. Rev. C **70**, 024002 (2004).
[16] C. Kurokawa and K. Katō, Phys. Rev. C **71**, 021301 (2005).
[17] K. Arai, Phys. Rev. C **74**, 064311 (2006).
[18] M. Theeten, H. Matsumura, M. Orabi, D. Baye, P. Descouvemont, Y. Fujiwara, and Y. Suzuki, Phys. Rev. C **76**, 054003 (2007).
[19] C. Kurokawa and K. Katō, Nucl. Phys. A **792**, 87 (2007).
[20] P. Descouvemont and D. Baye, Phys. Rev. C **36**, 54 (1987).
[21] M. Orabi, Y. Suzuki, H. Matsumura, Y. Fujiwara, D. Baye, P. Descouvemont, and M. Theeten, J. Phys. Conf. Ser. **111**, 012045 (2008).
[22] Y. Suzuki, H. Matsumura, M. Orabi, Y. Fujiwara, P. Descouvemont, M. Theeten, and D. Baye, Phys. Lett. B **659**, 160 (2008).
[23] P. Descouvemont, J. Phys. G **37**, 064010 (2010).
[24] T. Yoshida, N. Itagaki, and K. Katō, Phys. Rev. C **83**, 024301 (2011).

[25] N. Moiseyev, Phys. Rep. **302**, 212 (1998).
[26] Y. K. Ho, Phys. Rep. **99**, 1 (1983).
[27] G. S. Anagnostatos, Phys. Rev. C **51**, 152 (1995).
[28] A. C. Merchant and W. D. M. Rae, Nucl. Phys. A **549**, 431 (1992).
[29] Y. Kanada-En'yo, Progr. Theor. Phys. **117**, 655 (2007).
[30] T. Neff and H. Feldmeier, Nucl. Phys. A **738**, 357 (2004).
[31] A. I. Baz', Soviet J. Exp. Theor. Phys. **43**, 205 (1976).
[32] T. Muñoz-Britton, M. Freer, N. I. Ashwood, T. A. D. Brown, W. N. Catford, N. Curtis, S. P. Fox, B. R. Fulton, C. W. Harlin, A. M. Laird, P. Mumby-Croft, A. S. J. Murphy, P. Papka, D. L. Price, K. Vaughan, D. L. Watson, and D. C. Weisser, J. Phys. G **37**, 105104 (2010).
[33] M. Freer, H. Fujita, Z. Buthelezi, J. Carter, R. W. Fearick, S. V. Förtsch, R. Neveling, S. M. Perez, P. Papka, F. D. Smit, J. A. Swartz, and I. Usman, Phys. Rev. C **80**, 041303 (2009).
[34] V. Vasilevsky, A. V. Nesterov, F. Arickx, and J. Broeckhove, Phys. Rev. C **63**, 034606 (2001).
[35] V. Vasilevsky, A. V. Nesterov, F. Arickx, and J. Broeckhove, Phys. Rev. C **63**, 034607 (2001).
[36] J. Broeckhove, F. Arickx, P. Hellinckx, V. S. Vasilevsky, and A. V. Nesterov, J. Phys. G **34**, 1955 (2007).
[37] V. Vasilevsky, F. Arickx, J. Broeckhove, and V. N. Romanov, Ukr. J. Phys. **49**, 1053 (2004).
[38] V. Vasilevsky, A. V. Nesterov, F. Arickx, and J. Broeckhove, Phys. Rev. C **63**, 064604 (2001).
[39] S. Korennov and P. Descouvemont, Nucl. Phys. A **740**, 249 (2004).
[40] A. Damman and P. Descouvemont, Phys. Rev. C **80**, 044310 (2009).
[41] Y. Fujiwara, Y. Suzuki, K. Miyagawa, M. Kohno, and H. Nemura, Prog. Theor. Phys. **107**, 993 (2002).
[42] Y. A. Lashko and G. F. Filippov, Nucl. Phys. A **826**, 24 (2009).
[43] W. Zickendraht, Ann. Phys. **35**, 18 (1965).
[44] J. Nyiri and Y. A. Smorodinsky, Yad. Fiz. **29**, 833 (1979).
[45] A. V. Nesterov, F. Arickx, J. Broeckhove, and V. S. Vasilevsky, Phys. Part. Nucl. **41**, 716 (2010).
[46] D. R. Thompson, M. LeMere, and Y. C. Tang, Nucl. Phys. A **286**, 53 (1977).
[47] A. Sytcheva, F. Arickx, J. Broeckhove, and V. S. Vasilevsky, Phys. Rev. C **71**, 044322 (2005).
[48] K. Wildermuth and Y. Tang, *A Unified Theory of the Nucleus* (Vieweg Verlag, Braunschweig, 1977).